

A Conceptual Study on Photodynamic Control-Mediated Holographic Composites

Yewon Lee, Hyeong Seok Kim, Yi Young Kang, Hye Ju Kang, Jieun Lee, Jawon Kim, Jae-Won Lee, Su-Won Lee, Seungah Min, Won-Gun Koh, Youngjong Kang, Hak-Rin Kim, and Jae-Won Ka*

Herein, photodynamic control-mediated holographic composites are proposed, which are composed of photosensitizers, singlet oxygen receptors, and a polymeric matrix. Rose bengal (RB) and methylene blue (MB) are used as photosensitizers, and 1,3-diphenylisobenzofuran (DPBF) as a singlet oxygen receptor. First, the photodynamic effects of the photosensitizers in DPBF-dissolved solutions are evaluated by analyzing the optical properties of DPBF under laser irradiation. The results confirm that RB and MB are selectively photoexcited by a green and red laser, respectively, and DPBF only reacts to the photosensitized singlet oxygen. Similarly, an outstanding photodynamic effect is observed in the DPBF-coated photodynamic films upon 660 nm laser irradiation. To evaluate the holographic performances of the films, the diffraction efficiency of the films is measured under the beams. The diffraction efficiency of the films is 2.03%. The results suggest that the conformational changes of the receptor are accompanied with absorptive gradients on the films. Therefore, it is strongly believed that the new strategy with photodynamic control can provide appealing solutions in the near future for holographic applications.

index patterns are efficiently created with high photosensitivity and large dynamic ranges during photopolymerization. Furthermore, a less complicated process is required for photopolymeric applications.^[4]

In principle, the process of monomeric diffusion should be involved in efficient holographic recordings, where the unreacted monomers in the less-exposed region should be transported to the brighter regions to compensate for concentration gradients.^[3a,5] However, during such an essential process, the volumetric shrinkage of the polymer coincides with diminished holographic performance.^[6] Several trials have been suggested for addressing the issue, that is, organic/inorganic hybrid matrix,^[4b] “Dewer” benzene with photo-conformational changes for non-diffusive holographic recordings.^[7] However, polymer matrices with a relatively low transition temperature (T_g)


should be considered to enable the facile diffusion of monomers in photopolymeric systems,^[5a] thereby limiting the required high-temperature applications. Therefore, new platforms with specific characteristics are required to overcome the limitations of previous holographic materials and exhibit enhanced holographic performances, regardless of advantages from photopolymeric system for holographic recordings.

1. Introduction

Holographic recordings are obtained as a result of the interference characteristics of light, providing 3D optical information.^[1] Notably, among several holographic materials such as silver halides^[2] and dichromated gelatin,^[3] photopolymers have been extensively investigated because their refractive

Y. Lee, H. S. Kim, Y. Y. Kang, H. J. Kang, J. Lee, J. Kim, S. Min, J.-W. Ka
Advanced Polymer Materials Research Center
Korea Research Institute of Chemical Technology
141 Gajeong-ro, Yuseong-gu, Daejeon 34114, Korea
E-mail: jwka@kriict.re.kr

Y. Lee, J. Kim, W.-G. Koh
Department of Chemical & Biomolecular Engineering
Yonsei University
50 Yonsei-ro, Seodaemun-gu, Seoul 03722, Korea

 The ORCID identification number(s) for the author(s) of this article can be found under <https://doi.org/10.1002/adpr.202100363>.

© 2022 The Authors. Advanced Photonics Research published by Wiley-VCH GmbH. This is an open access article under the terms of the Creative Commons Attribution License, which permits use, distribution and reproduction in any medium, provided the original work is properly cited.

DOI: 10.1002/adpr.202100363

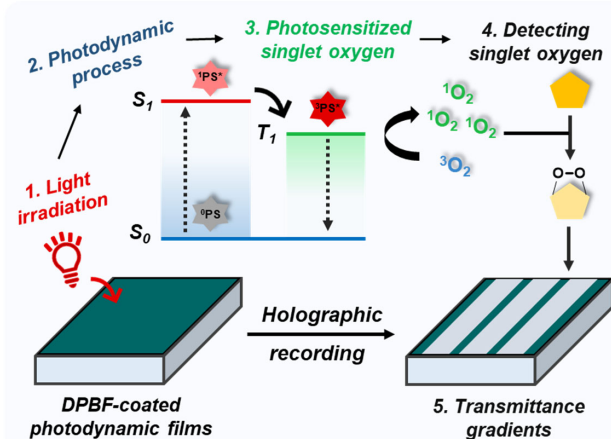
J.-W. Lee, S.-W. Lee, H.-R. Kim
School of Electronic and Electrical Engineering
Kyungpook National University
80 Daehak-ro, Buk-gu, Daegu 41566, Korea

S. Min, Y. Kang
Department of Chemistry
Hanyang University
222 Wangsimni-ro, Seongdong-gu, Seoul 04763, Korea

H.-R. Kim
School of Electronics Engineering
Kyungpook National University
80 Daehak-ro, Buk-gu, Daegu 41566, Korea

Photoexcited photosensitizers can generate singlet oxygen ($^1\text{O}_2$) by facilitating intersystem crossing, which is a transition from the singlet excited state (S_1) to the lowest triplet excited state (T_1).^[8] Owing to the severe reactivity of the formed singlet oxygen, photosensitizers play various roles in selectively killing cancer cells over normal cells (termed as “photodynamic therapy”),^[8a,9] oxidizing agents,^[9a] and destroying wastes.^[10] Therefore, it has been interesting to detect the singlet oxygen generated during the photodynamic process using chemical agents, such as 1,3-diphenylisobenzofuran (DPBF)^[11] and 9,10-diphenylanthracene (DPA).^[12] These agents have structural advantages that provide selectivity to singlet oxygen. Upon reaction with photosensitized singlet oxygen, the conformational changes of the detectors occur with diminished absorbance intensity.^[11,12] Apparently, such photo-controlled processes could induce transmittance gradients between the light-active and the light-inactive regions from the results of absorbance changes, appealing to a new type of holographic recording.

In this study, we propose photodynamic control-mediated holographic composites for recording holograms. This new system is composed of three parts: 1) photosensitizers for generating singlet oxygen, 2) receptors to scavenge the oxidant with optical changes, and 3) polymeric matrix for providing functionalities, such as solubility and heat resistance (Scheme 1), on the films. Upon light irradiation, photoexcited sensitizers can generate singlet oxygen. Owing to its short-lived characteristics,^[13] singlet oxygen can immediately react with the surrounding receptors. Then, the absorptive intensity of the receptors on the exposed films was significantly reduced, while no optical changes were observed on the unexposed films. These results could induce differences in optical properties, enabling the writing of interference patterns on the films for holographic recordings. Unlike conventional materials for holographic



Scheme 1. Schematic illustration of holographic composites with photodynamic controls. Upon light irradiation on the 1,3-diphenylisobenzofuran (DPBF)-coated photodynamic films, the singlet oxygen ($^1\text{O}_2$) is generated through a photodynamic process on the films. Thereafter, the receptors can instantly scavenge the photosensitized singlet oxygen with structural changes, resulting in the transmittance gradients on the films through reduced absorptive properties of DPBF for efficient holographic recordings. Consequently, holographic recordings are available on the photodynamic films mediated by the singlet oxygen detector.

recordings,^[4a,6c,14] which are composed of complex components, photoactive holographic films can be easily fabricated with functionalities such as better solubility, heat resistance, and flexibility, potentiating to various holographic applications. Furthermore, the shrinkage issues that are induced from consumed monomeric concentration during photopolymerization of the conventional method could be inherently avoided, by using simple photodynamic combinations, instead of monomers. To the best of our knowledge, this is the first report on photodynamic control-mediated holographic materials with holographic performances.

2. Results and Discussion

2.1. Design of Photodynamic Control-Mediated Holographic Composites

To avoid the disadvantages of previous holographic materials, we introduced photodynamic components in polymeric composites consisting of a photosensitizer/singlet oxygen receptor with a matrix (binder). As a proof of concept, the singlet oxygen generated during the photodynamic process converted the conformations of the receptors with absorptive changes, thereby making the transmission gradients for writing holographic images (Figure 1A). Rose bengal (RB) and methylene blue (MB) were used as photosensitizers with different photoactive wavelengths (532 and 660 nm) to confirm photodynamic behaviors in the green and red regions, respectively. In addition, DPBF was utilized to detect singlet oxygen ($^1\text{O}_2$) generated by the aforementioned sensitizers in a poly(methyl methacrylate) (PMMA) matrix, demonstrating better solubility of the entire system.

2.2. Photodynamic Behaviors of a Combination of Photosensitizers/singlet Oxygen Receptors

To demonstrate the photodynamic behavior of new composites, we prepared compositions of photosensitizers and singlet oxygen receptors to a solution of organic solvents and measured their optical properties.

First, the absorbances of RB and MB were analyzed to determine the proper photoactive wavelengths. The maximum absorptive intensities of RB and MB were observed at 563 and 665 nm, respectively (Figure S1, Supporting Information). Considering that these absorbances significantly were overlapped with the laser wavelength of 532 and 660 nm, it is strongly estimated that the efficient photodynamic effect of sensitizers can be seen under light irradiation.

In the case of DPBF, which is a common substance that reacts with singlet oxygen,^[11] the inherent absorbance was observed at ≈ 415 nm, emitting bright blue fluorescence under ultraviolet (UV) light (Figure S2, Supporting Information). A solution of DPBF was irradiated for 60 min. Regardless of green or red light irradiation, negligible changes were observed (Figure S2, Supporting Information). This indicates that DPBF can only react with photosensitized singlet oxygen without further perturbation by exposure to light.

Owing to the specific reactivity of the receptors, DPBF was combined with RB in organic solutions to confirm its

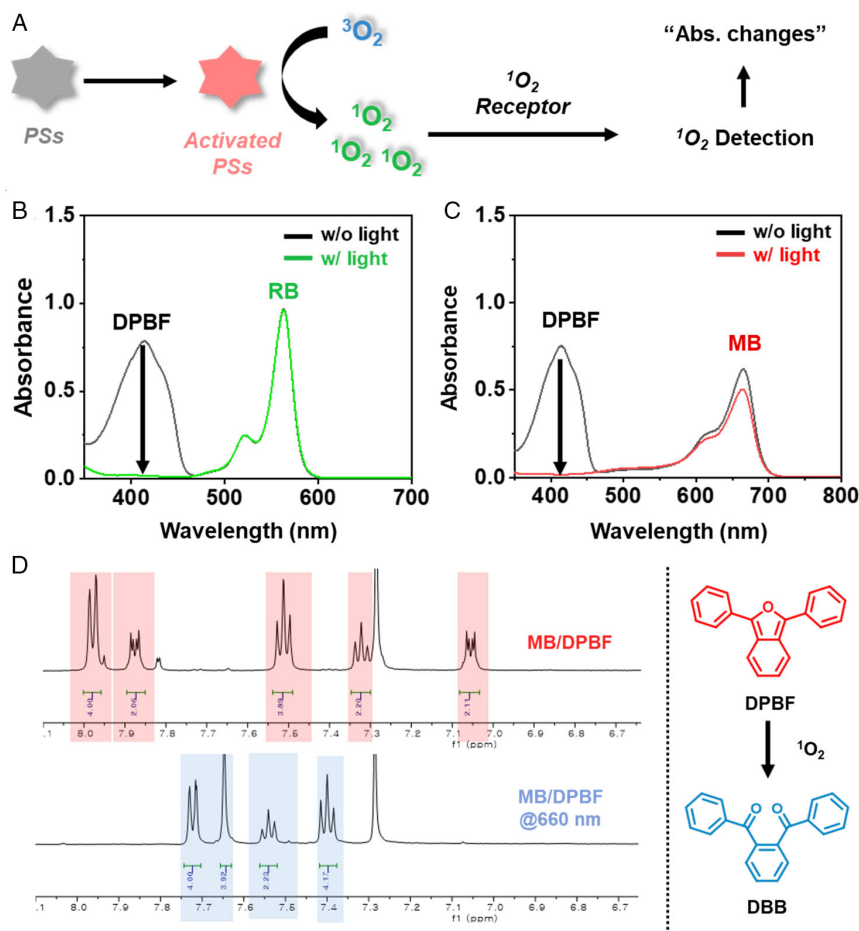


Figure 1. Photodynamic behavior of photosensitizers/singlet oxygen receptors in solutions. A) Schematic illustration of the photodynamic mechanism of photosensitizers and the detection of photosensitized singlet oxygen by the receptors. B) Absorbance spectra of 1,3-diphenylisobenzofuran (DPBF) in B) rose bengal (RB)- and C) methylene blue (MB)-dissolved solutions. RB and MB were photoexcited at 532 and 660 nm, respectively. Then, absorbance spectra of DPBF were recorded after light irradiation for 10 s. D) Proton nuclear magnetic resonance (^1H NMR) spectra to confirm the mechanism that photosensitized singlet oxygen is detected by DPBF with structural changes. Red and blue highlighted regions refer to peaks of DPBF and DBB, respectively. Upper: MB/DPBF in solution. Below: MB/DPBF after light irradiation (660 nm) for 30 min.

photodynamic behavior. After the solution was irradiated with a 532 nm laser for 10 s (Figure 1B), the absorbance of DPBF was completely diminished. Furthermore, its fluorescence intensity was reduced under 365 nm (Figure S2, Supporting Information), resulting from structural changes of DPBF by the formation of singlet oxygen from photoactivated sensitizers.

Next, we used MB as a photosensitizer in the dissolved DPBF solution. The maximum absorbance intensity of MB was observed at 665 nm (Figure S1, Supporting Information); hence, it was suggested that MB is a suitable candidate for generating singlet oxygen under red laser irradiation. Thus, upon 660 nm light irradiation, the absorbance of DPBF was gradually reduced, probing the photodynamic behavior of the photosensitizer within the MB/DPBF solution. Furthermore, as supporting evidence, proton nuclear magnetic resonance (^1H NMR) analyses were performed to verify the photodynamic behavior of the new system. Upon light irradiation of the MB/DPBF solution, the aromatic peaks of DPBF disappeared, generating new DBB peaks (Figures 1D and S3, Supporting Information). These results

demonstrate that a new type of polymeric composite with photodynamic effects could enable the recording of 3D images in the irradiation of green and red lasers.

2.3. Preparation of DPBF-Coated Photodynamic Films and Evaluation of Photodynamic Behaviors

To verify our conceptual studies for holographic recording, we fabricated photodynamic films with photosensitizers/singlet oxygen receptors/PMMA matrix (Figure 2A). First, the mixtures of each sensitizer (RB and MB) and DPBF were dissolved in organic solvents. Thereafter, these solutions were spin-coated onto the PMMA matrix using a dry process. The resultant films exhibited blue/green colors (Figure S4, Supporting Information) with averaged thickness of $\approx 7.24 \mu\text{m}$ (Figure S5, Supporting Information).

After preparing the DPBF-coated photoactive films (RB/DPBF/PMMA and MB/DPBF/PMMA), we measured the

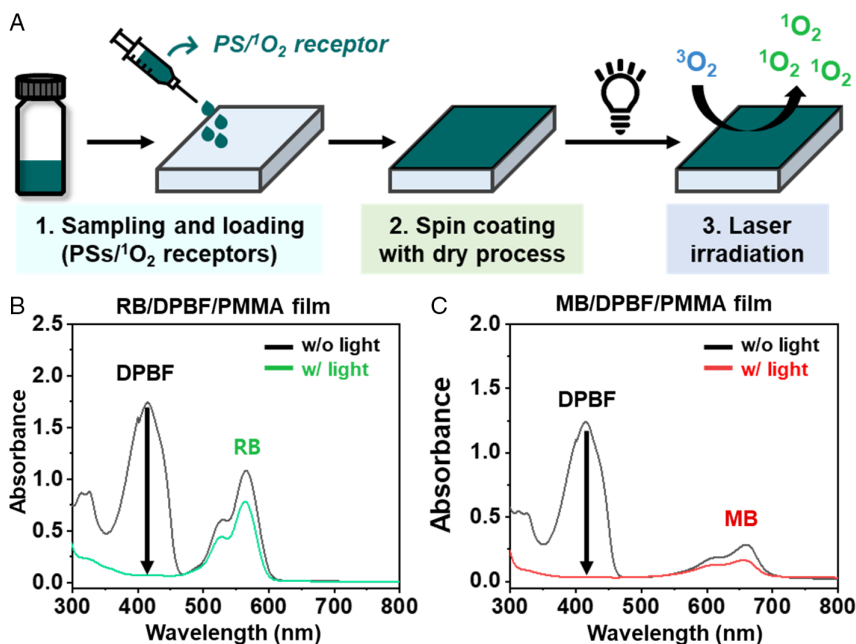


Figure 2. Photodynamic behavior of photosensitizers/singlet oxygen receptor in films. A) Schematic illustration of the fabrication of the DPBF-coated photodynamic films. Absorbance spectra of DPBF in B) RB- and C) MB-loaded films under laser irradiation. RB and MB were photoexcited at 532 and 660 nm, respectively. Thereafter, the absorbance spectra of DPBF were recorded after light irradiation for 5 min.

photodynamic behavior of the films. Considering that the photosensitizers have a specific wavelength to generate singlet oxygen (Figure S1, Supporting Information), RB and MB were irradiated at 532 and 660 nm, respectively. As a result, the absorbance peaks of DPBF in both films gradually decreased upon light irradiation (Figure 2B,C). In contrast, negligible changes in absorbance for the light irradiation of 532 and 660 nm were observed in the case of DPBF-loaded films (DPBF/PMMA, Figure S7, Supporting Information) without photosensitizers. These results strongly support the specific reactivity of DPBF to photosensitized singlet oxygen without perturbation by light.

2.4. Patterning Tests on MB/DPBF/PMMA Film Under Laser Irradiation of 660 nm

Patterning tests were performed to confirm that the patterns on the films were written by the photodynamic control. Owing to the outstanding photodynamic properties of MB/DPBF films, we decided to use the MB/DPBF/PMMA film as a patterning platform.

After preparing the MB-loaded films, we covered the films with silver foils in the shape of letter “K.” Thereafter, the films were irradiated with a 660 nm laser. As a result, the color of the films changed from green/blue to colorless (Figure 3, upper). Owing to the reaction between DPBF and photosensitized singlet oxygen, the fluorescence of DPBF was diminished in “K” shape on the films. When the foils were uncovered, the inherent color of the film was observed in the unexposed region, emitting strong fluorescence of DPBF under UV light (Figure 3, below). In contrast, negligible optical changes were observed in the case of the DPBF-coated films, regardless of green and red laser irradiations (Figure S8, Supporting Information). Furthermore, upon light irradiation, the patterns on the PMMA-composed

films were maintained without light-induced perturbation (Figure S9, Supporting Information). These results could guarantee the writable performance of the DPBF-coated films with a photodynamic process for holographic recording.

2.5. Measurement of the Diffraction Efficiency (η) of Photodynamic Films to Evaluate Holographic Performances

The diffraction efficiency (η) is defined as a ratio of the diffracted and incident intensities of the probe beam on the gratings, and it has been a key factor of determining holographic performances.^[4a,14a,d,15] Therefore, we measured the diffraction efficiency of the photodynamic films (MB/DPBF/PMMA) to evaluate their holographic writing performances. For the experimental setting, a 660 nm laser as a writing beam, the most appropriate photoexcitation light of MB, and blue laser as a reference beam were irradiated. Upon light irradiation, the writing beam was split into two beams, forming interference patterns at an angle of 13° (Figure S10, Supporting Information). After calculating the optical powers of the diffracted/incident beams, the maximum diffraction efficiency of the film was recorded as 4.42% within ≈ 200 s of recording time. However, the efficiency gradually saturated at 2.03% after 2500 s (Figure 4). It was estimated that the absorptive properties of DPBF on the films were immediately reduced owing to the relatively high intensity of the blue probe beam, ultimately inducing less holographic performance. Nevertheless, this result is significantly comparable to that of a previous study on transmittance-type holographic grafting.^[14d] Therefore, the new photodynamic composites in this work could provide achievable solutions to overcome some of the limitations of conventional holographic materials.

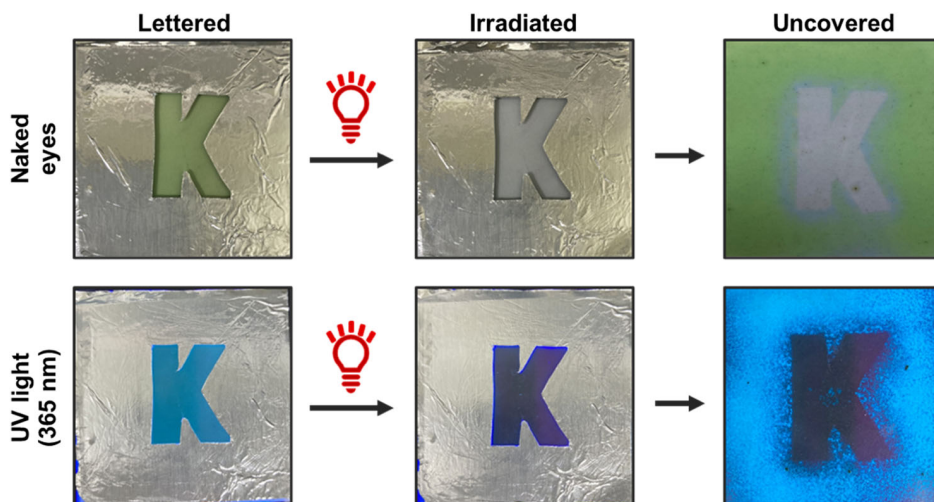


Figure 3. Patterning tests of the MB/DPBF/PMMA films under 660 nm light irradiation. The films with the K-shaped pattern were irradiated with 660 nm laser for 30 min. Upper: images of the photodynamic films visible to naked eyes. Below: fluorescence images of DPBF under UV light irradiation.

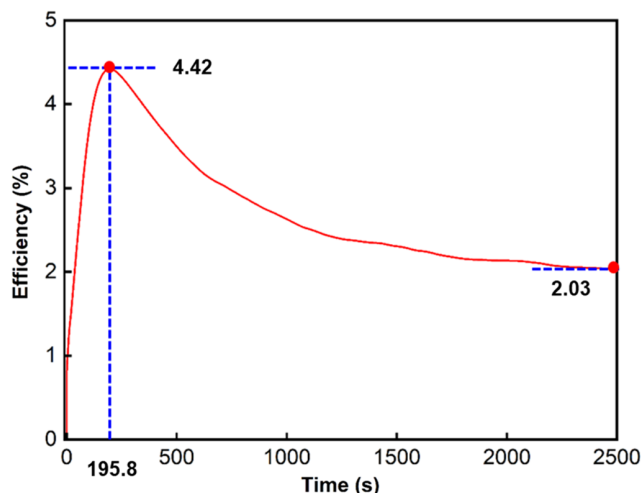


Figure 4. Diffraction efficiency (η) of the MB/DPBF/PMMA films. The diffraction efficiency was calculated as $\eta(\%) = \frac{2I_d}{I_i} \times 100$, where I_d is the intensity of the diffraction beam of order + 1, and I_i is the intensity of the probing beam.

3. Conclusions

Herein, we proposed a new holographic composite with photodynamic control, composed of photosensitizers, singlet oxygen receptors, and polymeric binders. Upon laser irradiation, photoexcited sensitizers can generate singlet oxygen, which can be detected by their receptors through changes in absorptive properties. Such photoactive changes within holographic composites could cause permanent interference by light-induced transmittance gradients, ultimately enabling holographic recordings.

In this study, we used RB and MB as photosensitizers, DPBF as a singlet oxygen receptor, and PMMA matrix to obtain a better soluble system. After measuring the optical properties of the components in the new system, we confirmed that 1) RB and MB were properly photoactivated by green and red lasers, respectively, and 2) DPBF only reacted with the photosensitized singlet oxygen.

Therefore, we fabricated DPBF-coated photoactive films on a PMMA matrix using a facile process—spin-coating. In the case of the MB/DPBF film, reliable photodynamic behavior was observed with only patterning results on the exposed region upon laser irradiation of 600 nm. Further, as an important factor for efficient holographic recordings, the diffraction efficiency of the DPBF-coated films was recorded as 2.03%, which is comparable to that of transmittance-type systems reported in a previous study.

Although considerable holographic performance was evaluated in the newly proposed holographic composites, some requirements should be considered to enhance the photodynamic performance of the films. For example, light-stable photosensitizers with better solubility must be used to evaluate the photodynamic effects of the new composites. Owing to the slight degradation of RB and MB upon light irradiation (Figure S6, Supporting Information), the inherent photodynamic behaviors of the photosensitizers could be inhibited. Furthermore, during the preparation of the solution and films, all the components were not sufficiently soluble. It is probable that the photodynamic behavior of a new system and its diffraction efficiency are not appropriately proven. Thus, optimal combinations of photosensitizers/ROS receptors should be investigated for a range of holographic applications to prevent undesirable results.

Currently, we are planning to introduce more proper photosensitizers and receptors for new holographic composites and thus determine optimized compositions with no further concerned limitations. In addition, benefiting from the utilization of functional binders in the new system, we are designing new photodynamic films with new characteristics such as heat resistance and flexibility to enable several holographic applications. We believe that our new strategy can provide motivation and ideas for efficient holographic recordings in the near future.

4. Experimental Section

Materials and Instrumentations: All the reagents and solvents used in this study were purchased from Sigma–Aldrich: RB (95%,

Sigma-Aldrich), MB ($\geq 82\%$, Sigma-Aldrich), DPBF (97%, Sigma-Aldrich), PMMA (molecular weight: $\approx 120\,000$, Sigma-Aldrich), dimethylformamide (DMF, 99.8%, Sigma-Aldrich), chloroform (99%, Sigma-Aldrich), tetrahydrofuran (THF, 99.9%, Sigma-Aldrich), and CDCl_3 (99.8 atm% of D, 0.5 wt% of silver foil as stabilizer, Sigma-Aldrich). Except for DPBF, all reagents and solvents were used without any further purification. DPBF was purified using column chromatography (silica gel [230–400 mesh], Merck).

For photoexcitation of the photosensitizers with a power of 50 mW cm^{-2} , MGL-FN-532 (532 nm, maximum intensity = 0.5 W cm^{-2} , CNI Optoelectronics Technology Co., Ltd.) and MDL-III-660 (660 nm, maximum intensity = 0.5 W cm^{-2} , CNI Optoelectronics Technology Co., Ltd.) lasers were used. Absorption spectra were measured using a PerkinElmer Lambda 365 UV–vis spectrophotometer at room temperature with a 1 cm quartz cuvette. ^1H NMR spectra were measured using a Bruker NMR spectrometer (400 and 500 MHz).

Preparation of a Solution of Photosensitizers and Singlet Oxygen Receptors: By blocking the light, RB (7.53 μM) and MB (7.53 μM) were individually added to the solutions of DPBF (30.1 μM) in DMF. The photosensitizers were irradiated with light (50 mW cm^{-2}) for 10 s, and their absorbance spectra were recorded to evaluate their photodynamic effects. Additionally, DPBF (45.2 μM) in a solution of DMF was irradiated at 532 and 632 nm for 5 min.

NMR Analysis: The solution of MB (100 mM) and DPBF (100 mM) in CDCl_3 was prepared and its ^1H NMR spectrum was recorded. Upon 660 nm laser irradiation for 30 min, new proton peaks were observed. The NMR analyses were conducted in a dark room to avoid undesired light degradation of the reagents.

Preparation of DPBF-Coated Photodynamic Films: In the dark room, PMMA (499 mg, 18.05 wt%) was added to a solution of RB (10.7 mg, 0.39 wt%) and DPBF (34.8 mg, 1.26 wt%) in 2.5 mL of THF, and the mixture was stirred at 50°C for 1 h. This mixture was spin-coated at 1000 rpm for 10 s and then dried at 50°C . Thereafter, for the fabrication of MB/DPBF/PMMA films, MB (4.1 mg, 0.10 wt%) and DPBF (34.5 mg, 0.81 wt%) were dissolved in 2.5 mL of chloroform (2.5 mL) with the PMMA (499 mg, 11.69 wt%) and stirred at 50°C for 1 h. The solution was spin-coated at 1000 rpm for 10 s and then dried at 50°C . The photodynamic behaviors of the films were evaluated under laser irradiation.

Patterning Experiments: For the patterning tests, we first prepared MB/DPBF-coated films with PMMA. To a solution of MB (27.2 mg, 0.63 wt%) and DPBF (34.5 mg, 0.81 wt%) (MB:DPBF = 1:1.5 molar ratio), PMMA (499 mg, 11.64 wt%) was added and stirred at 50°C under dark condition for 1 h. The solution was spin-coated at 1000 rpm for 10 s and then dried at 50°C . Further, the films were covered with silver foils in “K” shape. Upon 660 nm laser irradiation for 30 min, the optical properties of DPBF in the light-exposed “K” shape were diminished, forming the patterns.

Experimental Setup for Measuring Diffraction Efficiency (η): Lasers of wavelengths 660 nm (Cobolt Flamenco, Cobolt Ltd.) and 457 nm (Cobolt Twist, Cobolt Ltd.) were used as writing and probing beams, respectively. First, the 660 nm laser beam was split into two writing beams passing through the beam splitter to form an interference pattern with an interference angle of 13° on the film sample. These two beams were linearly polarized in the same direction to induce the amplitude for the interference patterns. In this system, the diffraction efficiency (η) was measured using the probing beam (457 nm laser) and two photodiodes. The intensity of the probing beam from the opposite side of the writing beam was measured by photodiode-1, as shown in Figure S9, Supporting Information. With further development of the interference patterns, the probing beam began to diffract, and the intensity of the diffracted beam with an order of +1 was measured in real time by photodiode-2. Finally, the diffraction efficiency of photodynamic films was derived as $\eta(\%) = \frac{2I_d}{I_i} \times 100$, where η is the diffraction efficiency, I_d is the intensity of the diffracted beam, and I_i is the intensity of the probing beam.

Supporting Information

Supporting Information is available from the Wiley Online Library or from the author.

Acknowledgements

Y.L. and H.S.K. contributed equally to this work. This work was supported by the Technology Innovation Industrial Program funded by the Ministry of Trade, Industry & Energy (10052667, Korea) and the KRICT Core Project (SS2021-20).

Conflict of Interest

The authors declare no conflict of interest.

Data Availability Statement

The data that support the findings of this study are available in the supplementary material of this article.

Keywords

holographic recordings, photodynamic effects, photodynamic films, photosensitizers, singlet oxygen receptors

Received: December 2, 2021

Revised: March 4, 2022

Published online: March 30, 2022

- [1] a) C. Jang, C. K. Lee, J. Jeong, G. Li, S. Lee, J. Yeom, K. Hong, B. Lee, *Appl. Opt.* **2016**, *55*, A71; b) J. S. Chen, D. P. Chu, *Opt. Express* **2015**, *23*, 18143; c) J. Ballato, T. Hawkins, P. Foy, B. Yazgan-Kokuoz, R. Stolen, C. McMillen, N. K. Hon, B. Jalali, R. Rice, *Opt. Express* **2009**, *17*, 8029.
- [2] P. Mas-Abellán, R. Madrigal, A. Fimia, *Proc. SPIE* **2019**, *11030*, 110301F.
- [3] a) J. C. Newell, L. Solymar, A. A. Ward, *Appl. Opt.* **1985**, *24*, 4460; b) J. Oliva, A. Fimia, J. A. Quintana, *Appl. Opt.* **1982**, *21*, 2891.
- [4] a) M. Ni, G. Chen, Y. Wang, H. Peng, Y. Liao, X. Xie, *Compos. B. Eng.* **2019**, *174*, 107045; b) S. Lee, Y.-C. Jeong, Y. Heo, S. I. Kim, Y.-S. Choi, J.-K. Park, *J. Mater. Chem.* **2009**, *19*, 1105; c) S. Lee, Y.-C. Jeong, J. Lee, J.-K. Park, *Opt. Lett.* **2009**, *34*, 3095; d) J. Yong-Cheol, S. Lee, J.-K. Park, *Opt. Express* **2007**, *15*, 1497.
- [5] a) K. Curtis, L. Dhar, A. Hill, W. Wilson, M. Ayres, *Holographic Data Storage: From Theory To Practical Systems*, Wiley, Hoboken, NJ **2010**; b) T. Mizuno, T. Goto, M. Goto, K. Matsui, T. Kubota, *Appl. Opt.* **1990**, *29*, 4757.
- [6] a) M. Moothanchery, I. Naydenova, V. Toal, *Appl. Phys. A* **2011**, *104*, 899; b) J. T. Gallo, C. M. Verber, *Appl. Opt.* **1994**, *33*, 6797; c) R. Fernández, S. Gallego, V. Navarro-Fuster, C. Neipp, J. Francés, S. Fenoll, I. Pascual, A. Beléndez, *Opt. Mater. Express* **2016**, *6*, 3455.
- [7] A. Khan, G. D. Stucky, C. J. Hawker, *Adv. Mater.* **2008**, *20*, 3937.
- [8] a) S. Wang, W. Wu, P. Manghni, S. Xu, Y. Wang, C. C. Goh, L. G. Ng, B. Liu, *ACS Nano* **2019**, *13*, 3095; b) W. Wu, X. Shao, J. Zhao, M. Wu, *Adv. Sci.* **2017**, *4*, 1700113; c) J. Zhao, W. Wu, J. Sun, S. Guo, *Chem. Soc. Rev.* **2013**, *42*, 5323; d) J. Martins, L. Almeida, J. Laranjinha, *Photochem. Photobiol.* **2004**, *80*, 267.
- [9] a) S. Xu, P. Zhou, Z. Zhang, C. Yang, B. Zhang, K. Deng, S. Bettle, H. Zhu, *J. Am. Chem. Soc.* **2017**, *139*, 14775; b) X. Ragas, X. He, M. Agut, M. Roxo-Rosa, A. R. Gonsalves, A. C. Serra, S. Nonell, *Molecules* **2013**, *18*, 2712.
- [10] L. Ville 'n, F. Manjo 'n, D. Garci 'a-Fresnadillo, G. Orellana, *Appl. Catal. B: Environ.* **2006**, *69*, 1.

- [11] T. Entradas, S. Waldron, M. Volk, *J. Photochem. Photobiol. B* **2020**, *204*, 1111787.
- [12] Q. Zheng, S. Jockusch, Z. Zhou, S. C. Blanchard, *Photochem. Photobiol.* **2014**, *90*, 448.
- [13] B. Marchetti, T. N. Karsili, *Chem. Commun.* **2016**, *52*, 10996.
- [14] a) Y.-X. Hu, X. Hao, L. Xu, X. Xie, B. Xiong, Z. Hu, H. Sun, G.-Q. Yin, X. Li, H. Peng, H.-B. Yang, *J. Am. Chem. Soc.* **2020**, *142*, 6285;
b) Y. Hu, B. A. Kowalski, S. Mavila, M. Podgorski, J. Sinha, A. C. Sullivan, R. R. McLeod, C. N. Bowman, *ACS Appl. Mater. Interfaces* **2020**, *12*, 44103; c) R. Fernandez, S. Bleda, S. Gallego, C. Neipp, A. Marquez, Y. Tomita, I. Pascual, A. Belendez, *Opt. Express* **2019**, *27*, 827; d) Y. Kobayashi, J. Abe, *Adv. Opt. Mater.* **2016**, *4*, 1354.
- [15] a) H. J. Kang, K.-I. Joo, Y. Y. Kang, J. Lee, Y. Lee, I. Jeon, T.-H. Lee, W.-G. Koh, J.-H. Choi, H.-R. Kim, J.-W. Ka, *Polym. J.* **2021**, *53*, 539;
b) Z. L. Deng, S. Zhang, G. P. Wang, *Nanoscale* **2016**, *8*, 1588;
c) W. C. Su, C. Y. Huang, J. Y. Chen, W. H. Su, *Opt. Lett.* **2010**, *35*, 405.